Further Experimental Studies of Two-Body Radiative Υ Decays

CLEO Collaboration

(February 7, 2008)

Abstract

Continuing our studies of radiative Υ decays, we report on a search for $\Upsilon \to \gamma\eta$ and $\Upsilon \to \gamma f_J(2220)$ in 61.3 pb^{-1} of e^+e^- data taken with the CLEO II detector at the Cornell Electron Storage Ring. For the $\gamma\eta$ search the three decays of the η meson to $\pi^+\pi^-\pi^0$, $\pi^0\pi^0\pi^0$, and $\gamma\gamma$ were investigated. We found no candidate events in the $(3\pi)^0$ modes and no significant excess over expected backgrounds in the $\gamma\gamma$ mode to set a limit on the branching fraction of $\mathcal{B}(\Upsilon \to \gamma\eta)<2.1\times10^{-5}$ at 90% C.L. The three charged two-body final states $h\overline{h}$ ($h = \pi^+, K^+, p$) were investigated for $f_J(2220)$ production, with one, one, and two events found, respectively. Limits at 90% C.L. of $\mathcal{B}(\Upsilon \to \gamma f_J) \times \mathcal{B}(f_J \to h\overline{h}) \sim 1.5 \times 10^{-5}$ have been set for each of these modes. We compare our results to measurements of other radiative Υ decays, to measurements of radiative J/ψ decays, and to theoretical predictions.

G. Masek,[1] H. P. Paar,[1] R. Mahapatra,[2] R. A. Briere,[3] G. P. Chen,[3] T. Ferguson,[3]
G. Tatishvili,[3] H. Vogel,[3] N. E. Adam,[4] J. P. Alexander,[4] C. Bebek,[4] K. Berkelman,[4]
F. Blanc,[4] V. Boisvert,[4] D. G. Cassel,[4] P. S. Drell,[4] J. E. Duboscq,[4] K. M. Ecklund,[4]
R. Ehrlich,[4] R. S. Galik,[4] L. Gibbons,[4] B. Gittelman,[4] S. W. Gray,[4] D. L. Hartill,[4]
B. K. Heltsley,[4] L. Hsu,[4] C. D. Jones,[4] J. Kandaswamy,[4] D. L. Kreinick,[4] A. Magerkurth,[4]
H. Mahlke-Krüger,[4] T. O. Meyer,[4] N. B. Mistry,[4] E. Nordberg,[4] M. Palmer,[4]
J. R. Patterson,[4] D. Peterson,[4] J. Pivarski,[4] D. Riley,[4] A. J. Sadoff,[4] H. Schwarthoff,[4]
M. R. Shepherd,[4] J. G. Thayer,[4] D. Urner,[4] B. Valant-Spaight,[4] G. Viehhauser,[4]
A. Warburton,[4] M. Weinberger,[4] S. B. Athar,[5] P. Avery,[5] H. Stoeck,[5] J. Yelton,[5]
G. Brandenburg,[6] A. Ershov,[6] D. Y.-J. Kim,[6] R. Wilson,[6] K. Benslama,[7] B. I. Eisenstein,[7]
J. Ernst,[7] G. D. Gollin,[7] R. M. Hans,[7] I. Karliner,[7] N. Lowrey,[7] M. A. Marsh,[7] C. Plager,[7]
C. Sedlack,[7] M. Selen,[7] J. J. Thaler,[7] J. Williams,[7] K. W. Edwards,[8] R. Ammar,[9]
D. Besson,[9] X. Zhao,[9] S. Anderson,[10] V. V. Frolov,[10] Y. Kubota,[10] S. J. Lee,[10] S. Z. Li,[10]
R. Poling,[10] A. Smith,[10] C. J. Stepaniak,[10] J. Urheim,[10] S. Ahmed,[11] M. S. Alam,[11]
L. Jian,[11] M. Saleem,[11] F. Wappler,[11] E. Eckhart,[12] K. K. Gan,[12] C. Gwon,[12] T. Hart,[12]
K. Honscheid,[12] D. Hufnagel,[12] H. Kagan,[12] R. Kass,[12] T. K. Pedlar,[12] J. B. Thayer,[12]
E. von Toerne,[12] T. Wilksen,[12] M. M. Zoeller,[12] S. J. Richichi,[13] H. Severini,[13] P. Skubic,[13]
S.A. Dytman,[14] S. Nam,[14] V. Savinov,[14] S. Chen,[15] J. W. Hinson,[15] J. Lee,[15]
D. H. Miller,[15] V. Pavlunin,[15] E. I. Shibata,[15] I. P. J. Shipsey,[15] D. Cronin-Hennessy,[16]
A.L. Lyon,[16] C. S. Park,[16] W. Park,[16] E. H. Thorndike,[16] T. E. Coan,[17] Y. S. Gao,[17]
F. Liu,[17] Y. Maravin,[17] I. Narsky,[17] R. Stroynowski,[17] J. Ye,[17] M. Artuso,[18]
C. Boulahouache,[18] K. Bukin,[18] E. Dambasuren,[18] R. Mountain,[18] T. Skwarnicki,[18]
S. Stone,[18] J.C. Wang,[18] A. H. Mahmood,[19] S. E. Csorna,[20] I. Danko,[20] Z. Xu,[20]
G. Bonvicini,[21] D. Cinabro,[21] M. Dubrovin,[21] S. McGee,[21] N. E. Powell,[21] A. Bornheim,[22]
E. Lipeles,[22] S. P. Pappas,[22] A. Shapiro,[22] W. M. Sun,[22] and A. J. Weinstein[22]

[1]University of California, San Diego, La Jolla, California 92093
[2]University of California, Santa Barbara, California 93106
[3]Carnegie Mellon University, Pittsburgh, Pennsylvania 15213
[4]Cornell University, Ithaca, New York 14853
[5]University of Florida, Gainesville, Florida 32611
[6]Harvard University, Cambridge, Massachusetts 02138
[7]University of Illinois, Urbana-Champaign, Illinois 61801
[8]Carleton University, Ottawa, Ontario, Canada K1S 5B6
and the Institute of Particle Physics, Canada M5S 1A7
[9]University of Kansas, Lawrence, Kansas 66045
[10]University of Minnesota, Minneapolis, Minnesota 55455
[11]State University of New York at Albany, Albany, New York 12222
[12]Ohio State University, Columbus, Ohio 43210
[13]University of Oklahoma, Norman, Oklahoma 73019
[14]University of Pittsburgh, Pittsburgh, Pennsylvania 15260
[15]Purdue University, West Lafayette, Indiana 47907
[16]University of Rochester, Rochester, New York 14627
[17]Southern Methodist University, Dallas, Texas 75275
[18]Syracuse University, Syracuse, New York 13244

[19]University of Texas - Pan American, Edinburg, Texas 78539

[20]Vanderbilt University, Nashville, Tennessee 37235

[21]Wayne State University, Detroit, Michigan 48202

[22]California Institute of Technology, Pasadena, California 91125

I. MOTIVATION

Exclusive radiative decays of the heavy vector states J/ψ and Υ have been the subject of many experimental and theoretical studies. For the experimenter, the final states from $V \rightarrow \gamma R$ are easy to identify and measure in that they have a high energy photon and low multiplicity of other particles. Backgrounds also tend to be small. Theoretically the emission of the photon leaves behind a glue-rich environment from which to learn about the formation of resonances from two gluons or to discover new forms of hadronic matter. Because gluons (g) themselves carry the quantum number of "color", QCD allows for states with *no* valence quarks (q), but only gluon constituents: "glueballs". QCD also allows for more exotic combinations such as $qg\overline{q}$ "hybrids". These glueballs and hybrids are not just more resonances in the spectrum - they represent fundamentally different forms of matter from the mesons and baryons with which we are so familiar.

For the J/ψ charmonium system (the 1_3S^1 state of $c\overline{c}$) many such radiative two-body decays have been observed [1], with some of the dominant ones being $\gamma f_2(1270)$, $\gamma\eta$, and $\gamma\eta'$. However, the only such observation in the radiative decay of the Υ (the 1_3S^1 state of $b\overline{b}$) is by CLEO [2] in the final state $\gamma\pi\pi$, in which an enhancement in the di-pion invariant mass consistent with being the $f_2(1270)$ meson was observed. A recent CLEO search [3] for the radiative production of the η' meson yielded only an upper limit.

In this Article we present a search for the radiative production of the other isoscalar pseudoscalar, namely the η meson. As with the final state $\gamma\eta'$, this channel has received significant theoretical attention. The work of Körner, Kühn, Krammer, and Schneider [4] and the followup publication by Kühn [5] use highly virtual gluons to predict minimal suppression of radiative pseudoscalar production as the vector meson mass goes from that of the J/ψ to that of the Υ. Intemann [6] used the vector dominance model (VDM) to predict branching fractions for $\Upsilon \rightarrow \gamma\eta$ taking into account the interference between the Υ and Υ', the major contributing vector mesons in the model. Baier and Grozin [7] showed that for lighter vector mesons (such as the J/ψ) there might be an additional "anomaly" diagram that contributes significantly to the radiative decays. Ball, Frère, and Tytgat worked along similar lines [8]. However, Baier and Grozin note that their approach applies directly to the "singlet" member of the meson nonet. Feldmann, Kroll, and Stech [9] pursue the ideas of mixing in the decay constants of the pseudoscalars to derive ratios of their radiative production. Chao [10] has taken this approach further, determining mixing angles such as $\lambda_{\eta\eta_b}$ between the η_b and η in order to calculate radiative branching fractions. Finally, the recent work of Ma Jian-Ping [11] uses factorization at tree level with non-relativistic QCD matrix elements to describe the heavy vector meson portion multiplied by a set of twist-2 and twist-3 gluonic distribution amplitudes.

The other search we present here is for the radiative production of the $f_J(2220)$, also known as the $\xi(2230)$, in Υ decay. Many theoretical calculations of the spectrum of glueballs predict a $J^{PC} = 2^{++}$ state in the area of 2.2 GeV/c^2. A candidate for this tensor glueball has been seen by some experiments, but not by others [1]. The most complete claim of observation is by the BES collaboration who have published results [12] for $J/\psi \rightarrow \gamma f_J(2220)$ with the $f_J(2220)$ reconstructed in $\pi^+\pi^-$, K^+K^-, $p\overline{p}$, and $K^0_S K^0_S$ as well as for $\pi^0\pi^0$ [13] and for $\eta\eta'$ [14]. Of significant interest are several non-observations. CLEO has not seen the f_J in two-photon interactions [15], which would lend credence to its being a glueball. However,

a narrow resonance in this mass region was not seen in $p\bar{p}$ production by either JETSET [16] or, more recently, by Crystal Barrel [17]. This non-observation sheds doubt on the very existence of the f_J.

II. DETECTOR AND DATA SAMPLE

Our analyses used 61.3 pb^{-1} of e^+e^- data recorded at the Υ(1S) resonance ($\sqrt{s} = 9.46$ GeV) with the CLEO II detector [18] operating at the Cornell Electron Storage Ring (CESR). This corresponds to the production of $N_\Upsilon = (1.45\pm0.03)\times10^6$ Υ(1S) mesons [2]. In addition, significantly larger samples taken near in time to this Υ(1S) data but at energies at or just below the Υ(4S) were used for comparison to the underlying continuum. The momenta and ionization loss (dE/dx) of charged tracks were measured in a six-layer straw-tube chamber, a ten-layer precision drift chamber, and a 51-layer main drift chamber, all operating in a 1.5 T solenoidal magnetic field. Photon detection and electron suppression were accomplished using the high-resolution electromagnetic calorimeter consisting of 7800 thallium-doped CsI crystals. The work presented here used only events with the primary, high-energy photon in the barrel portion of this detector, defined as $|\cos\theta| \le 0.71$, because the energy resolution for photons and reconstruction efficiency of the recoiling neutral mesons are degraded in the end cap regions and because the efficient, well understood triggers involve only the barrel region of the calorimeter. Between the central drift chamber and the electromagnetic calorimeter, strips of scintillating plastic were used for triggering and for measuring time-of-flight. Proportional tracking chambers for muon identification were located between and outside the iron slabs that provide the magnetic flux return. The Monte Carlo simulation of the detector response was based upon GEANT [19], and simulation events were processed in an identical fashion to data.

III. SEARCH FOR $\Upsilon \to \gamma\eta$

Our search for $\Upsilon \to \gamma\eta$ involved the decays $\eta \to \gamma\gamma$, $\eta \to \pi^0\pi^0\pi^0$, or $\eta \to \pi^+\pi^-\pi^0$; the latter two will collectively be referred to as $(3\pi)^0$. We followed procedures very similar to those used in our recent publication on the $\gamma\eta'$ final state [3]. In order to maximize detection efficiency and minimize possible systematic biases, we employed a minimal number of selection criteria, with combinatoric background largely suppressed by requiring reconstruction of both the Υ and η mesons.

Events were required to have the proper number of quality tracks (either zero or two) of appropriate charges and at least three calorimeter energy clusters (which may or may not be associated with the tracks), of which one had to correspond to an energy of at least 4 GeV and be in the barrel fiducial volume ($|\cos\theta| \le 0.71$). In addition, we required that the events pass trigger criteria [20], based purely on the calorimeter, that were highly efficient and could be reliably simulated.

For reconstructing π^0 candidates, the photon candidates had to have minimum deposi-

tions of 30 (50) MeV in the barrel (endcap) regions[1] and could not be associated with any charged track; in addition, at least one of the two photons had to be in the barrel region. The $\gamma\gamma$ invariant mass had to be within 50 MeV/c^2 ($\sim \pm 9\sigma_\pi$) of the known π^0 mass [1]; such candidates were then kinematically constrained to that mass. The photon candidates used in reconstructing the η meson in $\gamma\gamma$ had to deposit a minimum of 60 (100) MeV in the barrel (endcap) calorimeter regions, could not be identified as a fragment of a charged track deposition, and had to have a lateral profile consistent with that of a photon.

For the $\gamma(3\pi)^0$ modes we then built η candidates from $\pi^0\pi^0\pi^0$ or $\pi^+\pi^-\pi^0$. Simulation events were used to determine the detector mass resolution for these two signal modes: $\sigma_\eta = 10.7$ and 9.0 MeV/c^2, respectively. Candidates had to be within $\pm 3\sigma_\eta$ of the known η mass. In the case of the $\gamma\pi^0\pi^0\pi^0$ final state, no photon could be common to more than one π^0 combination. To suppress QED backgrounds in the $\gamma\pi^+\pi^-\pi^0$ final state, a charged track was rejected if its momentum, p, from the drift chamber matched its energy, E, as measured in the calorimeter as $0.85 < E/p < 1.05$.

Then, Υ candidates were formed by combining the high-energy photon ($E > 4$ GeV) with the η candidate, requiring that this photon not already be used in reconstructing the event. To be considered, such a candidate had to have an invariant mass within ± 300 MeV/c^2 of $\sqrt{s} = m_\Upsilon$, a window of roughly three times the detector resolution as obtained from our simulations. Although, in general, multiple candidates per event were not restricted, there were two exceptions: (i) in the case of $\eta \to \pi^0\pi^0\pi^0$, if two η candidates shared more than four photons, the candidate with the better combined χ^2 for mass fits to the three π^0 candidates was accepted; and (ii) in the case of $\eta \to \pi^+\pi^-\pi^0$, if two candidates for the neutral pion shared a daughter photon, the one with the better fit to the π^0 mass was taken.

After these highly-efficient procedures were applied, we found *no* candidates in either the 61.3 pb^{-1} of $\Upsilon(1S)$ data or in 189 pb^{-1} of continuum data samples.[2]

From Monte Carlo simulations, the overall efficiencies for each channel, ϵ_i, were determined to be $(7.6 \pm 0.8)\%$ and $(26.7 \pm 1.5)\%$ for the decay chains ending in $\eta \to \pi^0\pi^0\pi^0$ and $\eta \to \pi^+\pi^-\pi^0$, respectively. The uncertainties here include the statistics of the Monte Carlo samples and our estimates on possible systematic biases, which we discuss below. Including the branching fractions for the η decays [1] and their uncertainties gave $\sum[\epsilon_i \mathcal{B}_{\eta,i}] = (8.7 \pm 0.5)\%$ for $\Upsilon \to \gamma(3\pi)^0$.

For the final state $\gamma\gamma\gamma$, the significant QED background compelled us to change the order of the constraints on the meson reconstruction and to add one additional selection criterion. Here we *first* took three photons, as defined above, and required that $|m_{\gamma\gamma\gamma} - m_\Upsilon| \leq 300$ MeV/c^2. Then we took the photons in pairs and plotted the spectrum of $m_{\gamma\gamma}$.

A large background exists in both the $\Upsilon(1S)$ and $\Upsilon(4S)$ data sets, peaking near 0.40 GeV/c^2. From scanning such events it is evident that these are $e^+e^- \to \gamma\gamma$ events with pair

---

[1]The endcap region is defined as $0.85 < |\cos\theta| < 0.95$; the region between this and the barrel fiducial region is not used due to its poor resolution.

[2]While some of these data were at the $\Upsilon(4S)$ resonance, we note that B meson decays cannot have a high energy photon so that the analysis of these data yields only *udsc* or QED backgrounds.

production by one of the photons giving a final state of $\gamma e^+ e^-$. Tracks were not reconstructed in this subset of events due to the timing characteristics of the energy-based triggers in CLEO II. Such conversion events have their showers separated only in azimuth, in that the lepton pair has zero opening angle and any observed separation is due only to the bending by the magnetic field. Therefore, to suppress this $\gamma e^+ e^-$ background, we removed events for which the angular separation in the calorimeter had no polar angle (θ) component.

To show that most of the remaining $\gamma\gamma\gamma$ background is of QED or continuum origin and not from the $\Upsilon(1S)$, we took the higher-energy data and performed the same analysis. We then subtracted this spectrum of $m_{\gamma\gamma}$ from the $\Upsilon(1S)$ spectrum, after scaling it by the relative integrated luminosity, the relative reconstruction efficiencies, and the relative production rates. The last of these is determined from *udsc* continuum simulations at the two energies, for which we counted the number of events having one two-photon combination with an invariant mass within $3\sigma_{\gamma\gamma}$ of m_η. The mass resolution of $\sigma_{\gamma\gamma} = 15.7$ MeV/c^2 is taken from simulation of signal events. The result of this subtraction is shown in Figure 1; the integral of the entries in this figure is 4.3 ± 9.4, consistent with zero.
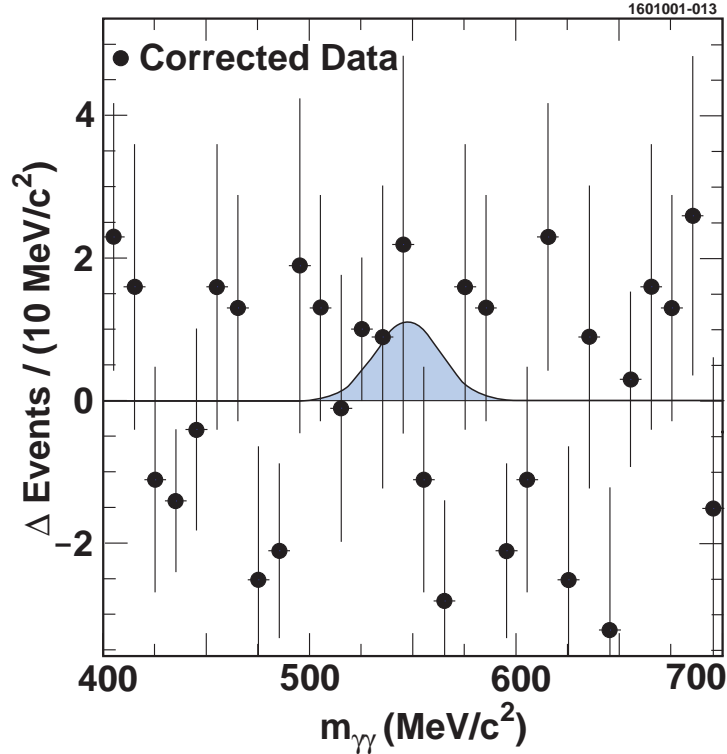

FIG. 1. Shown as solid circles is the di-photon spectrum for $\Upsilon(1S)$ data after subtraction of the $\Upsilon(4S)$ data, appropriately scaled. The $\Upsilon(1S)$ data are fit, using a likelihood technique, for a $\Upsilon(1S)\rightarrow\gamma\eta$ signal plus the scaled $\Upsilon(4S)$ spectrum, as detailed in the text. The superimposed curve shows the signal portion of the fit result.

We then performed a binned likelihood fit of the $\Upsilon(1S)$ data, using the value of the corresponding bin in the scaled distribution from the $\Upsilon(4S)$ data and a Gaussian signal function. Here the Gaussian had a mean of the established [1] value of the mass of the η meson and a width taken from our simulations of the signal ($\sigma_{\gamma\gamma} = 15.7$ MeV/c^2). The result

of the fit is shown in Figure 1, yielding 4.0±3.8 events. Bin-by-bin statistical variations in the $\Upsilon(4S)$ spectrum were taken into account by performing this procedure multiple times, each time randomly assigning the number of events in each $\Upsilon(4S)$ bin, according to the statistics of that bin. The distribution function used in determining the limit was the average of these several functions.

For this mode our overall reconstruction efficiency from signal simulation, including possible systematic biases and statistical uncertainties from the simulation, is $\epsilon_{\gamma\gamma} = (27.7\pm1.9)\%$.

The major sources of possible systematic uncertainty in our efficiency calculation for $\Upsilon \to \gamma\eta$ are shown in Table I. These follow closely those detailed in our prior study of $\Upsilon \to \gamma\eta'$ [3]. The degree of uniformity and definition of the fiducial volume of the barrel calorimeter (±2.2%) relates to our modeling the detector response to the proper angular distribution for this radiative Υ decay. Uncertainties in charged-track reconstruction (±1.0% per track), and trigger effects (±2.0%) were determined from previous detailed CLEO studies of low-multiplicity τ-pair and $\gamma\gamma$ events. Similar studies allowed determination of the possible uncertainty in the reconstruction of π^0 and η mesons from photons [21] (±3% per meson); this relates to our ability to find and measure the daughter photons and, in the case of the neutral pions, to have the two-photon invariant mass be within the $\pm9\sigma_\pi$ window around the established π^0 mass. Our ability to model the E/p requirement in the $\gamma\pi^+\pi^-\pi^0$ final state was assessed using charged pions from K_S^0 decays and assigned an uncertainty of ±3.2%. Shower leakage and other calorimeter effects make the mass distribution for Υ candidates asymmetric; based on CLEO experience with exclusive radiative B meson decays [22] we have assigned an uncertainty of ±2% regarding our ability to model these effects. Based on a study of varying the mass resolution, $\sigma_{\gamma\gamma}$, in fits to the data before all the final criteria were imposed, we assign a systematic uncertainty of ±5% from this source. These uncertainties were added in quadrature, along with the statistical uncertainty associated with the size of Monte Carlo samples, to obtain the overall systematic uncertainty in the efficiencies.

TABLE I. Systematic uncertainty contributions, as relative percentages, to the efficiency for the studied decay modes for $\Upsilon \to \gamma\eta$. The combined uncertainties were obtained using quadrature addition.

Uncertainty source	$\gamma\gamma$	$\pi^0\pi^0\pi^0$	$\pi^+\pi^-\pi^0$
Fiducial requirements	2.2	2.2	2.2
Track reconstruction	-	-	2.0
η, π^0 reconstruction from $\gamma\gamma$	3.0	9.0	3.0
E/p criterion	-	-	3.2
Trigger simulation	2.0	2.0	2.0
Υ mass distribution	2.0	2.0	2.0
Variation of $\sigma_{\gamma\gamma}$ in the fit	5.0	-	-
Monte Carlo statistics	1.6	2.4	1.0
Combined uncertainty	7.0	10.0	6.0

The systematic uncertainties and the statistical uncertainty in the number of $\Upsilon(1S)$ decays are incorporated by a Monte Carlo procedure to obtain likelihood distributions for

the branching fraction in each mode as $\mathcal{B}(\Upsilon \to \gamma\eta) = N_\eta/(\epsilon N_\Upsilon)$. In this approach we produce multiple experiments with N_η from the likelihood function appropriate for each decay mode[3] and then divide by an efficiency and by a number of $\Upsilon(1S)$ events, each picked from a Gaussian distribution about their mean values with the appropriate standard deviations. Summing the resulting likelihood distributions, as shown in Figure 2, to 90% of their areas resulted in limits for $10^5 \times \mathcal{B}(\Upsilon \to \gamma\eta)$ of 28.2, 6.7, 2.6, 1.9, and 2.1 for $\gamma\gamma\gamma$, $\gamma\pi^0\pi^0\pi^0$, $\gamma\pi^+\pi^-\pi^0$, $\gamma(3\pi)^0$, and all combined, respectively. The number of observed events, detection efficiencies and limits are presented in Table II.

TABLE II. Results for the search of $\Upsilon \to \gamma\eta$. Results include statistical and systematic uncertainties, as described in the text.

	$\gamma\gamma$	$\pi^0\pi^0\pi^0$	$\pi^+\pi^-\pi^0$
observed events	4.0 ± 3.8	0	0
$\mathcal{B}_{\eta,i}$ (%)	39.2 ± 0.3	32.2 ± 0.4	23.1 ± 0.5
Reconstruction efficiency (%)	27.7 ± 1.9	7.6 ± 0.8	26.7 ± 1.5
$\mathcal{B}(\Upsilon \to \gamma\eta)$ (90% C.L.)	$< 28.2 \times 10^{-5}$	$< 6.7 \times 10^{-5}$	$< 2.6 \times 10^{-5}$
Combined result	$< 2.1 \times 10^{-5}$		

To show that we could use CLEO data to observe π^0 and η mesons we also applied our same selection criteria, with the exception of requiring a high energy photon, to samples taken at the $\Upsilon(1S)$ and at or near the $\Upsilon(4S)$. Figure 3 shows examples of inclusive yields of η mesons in the $\Upsilon(4S)$ data that are consistent with the expected rates [1].

IV. SEARCH FOR $\Upsilon \to \gamma$ $\mathbf{F}_J(2220)$

Our search for $\Upsilon \to \gamma f_J(2220)$ used the three decay chains observed by BES [12] that involve two charged tracks: $f_J \to \pi^+\pi^-$, $f_J \to K^+K^-$, and $f_J \to p\overline{p}$. We followed procedures very similar to those used in our publication on the observation [2] of two-body radiative decays in $\Upsilon \to \gamma\pi\pi$.

Events were required to have two quality tracks of opposite charge with one energy deposition in excess of 4 GeV in the barrel fiducial volume ($|\cos\theta| \leq 0.71$) of the detector. The events were also required to pass trigger requirements [20] that were highly efficient for this process and that could be reliably simulated.

Backgrounds from QED processes such as $\gamma(\gamma)\mu^+\mu^-$ and $\gamma(\gamma)e^+e^-$ are potentially large, so we next imposed criteria to minimize them. At least one of the charged tracks had to extrapolate to the barrel muon detector and have momentum above 1.0 GeV/c and yet *not* be identified as a muon. For *each* track the ratio of calorimeter energy to its measured

---

[3]For the two $3(\pi)^0$ modes, which have no events actually observed, this likelihood function is a falling exponential as according to Poisson statistics.
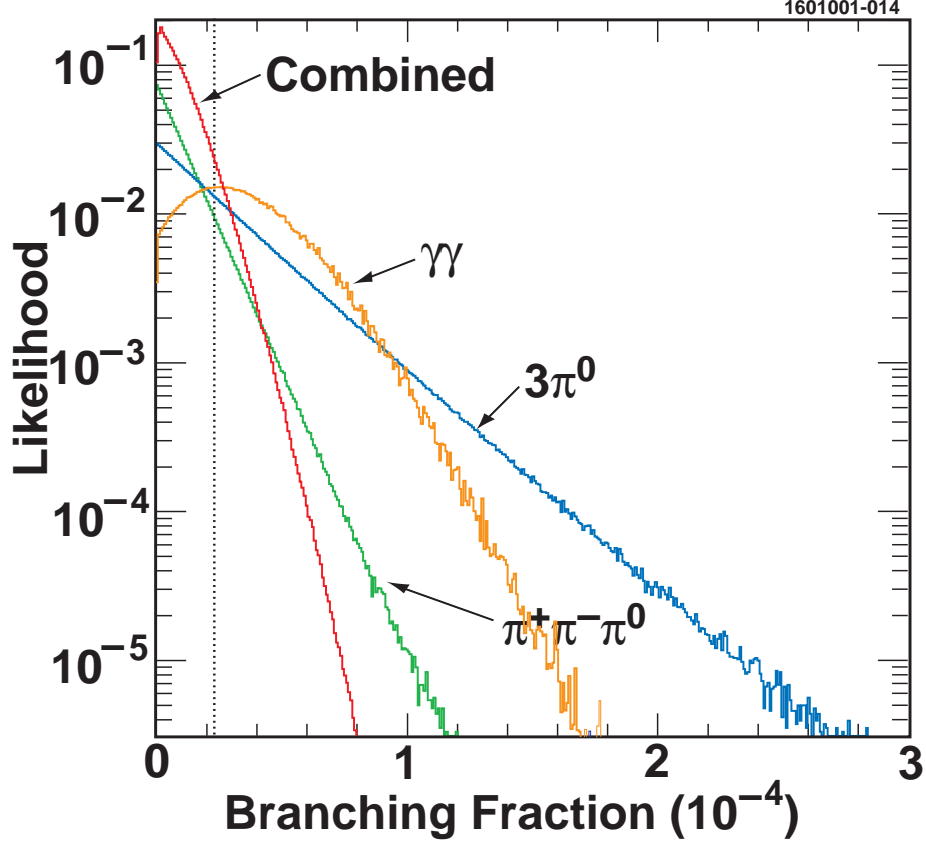
FIG. 2. Likelihood functions for branching fraction from the three final modes studied in our analysis and the combined likelihood function. All distributions include smearing by systematic uncertainties and have been normalized to unit area. The dotted vertical line is at 90% of the area of the combined function, namely 2.1×10^{-5}.

momentum had to satisfy $E/p < 0.85$ or $E/p > 1.05$, *i.e.,* inconsistent with that expected for an electron. The tracks could not be consistent with coming from a photon conversion and had to have an opening angle between them of less than 162°. For each of the three decay modes ($h = \pi^+, K^+, p$) we established four-momentum conservation by demanding $-0.03 < (E_{\gamma h \bar{h}} - \sqrt{s})/\sqrt{s} < 0.02$ and $|\vec{p}_{\gamma h \bar{h}}| < 150$ MeV/c; these represent approximately $\pm 3\sigma$ in our detector resolution and take into account the effect of initial state radiation. We did not explicitly reject multiple combinations per event, and none were observed in our simulations of the signal. For each of the three modes we then plotted the di-hadron invariant mass, as shown in Figure 4. In that we will be comparing our results to those of BES [12], we use a mass of $m_f = 2.234$ GeV/c^2 and a natural width of $\Gamma_f = 17$ MeV/c^2 for the f_J resonance. Our "signal box" is defined as $\pm 2\Gamma_f$ centered at m_f. For comparison, our signal simulations indicated mass resolutions (σ) of 15.6 ± 0.9, 14.8 ± 0.6, and 9.9 ± 0.4 MeV/c^2 for the final states $\pi^+\pi^-$, K^+K^-, and $p\bar{p}$, respectively.

The dominant continuum process ending in $\gamma\pi^+\pi^-$ is $e^+e^- \rightarrow \gamma\rho$. We used this reaction in two ways. First, we repeated the prior analysis of two-body radiative decays [2] to show that we could reproduce the shape and magnitude of the $\gamma\rho$ enhancement. To help us understand backgrounds we also studied data taken with an integrated luminosity of 838 pb^{-1} at energies
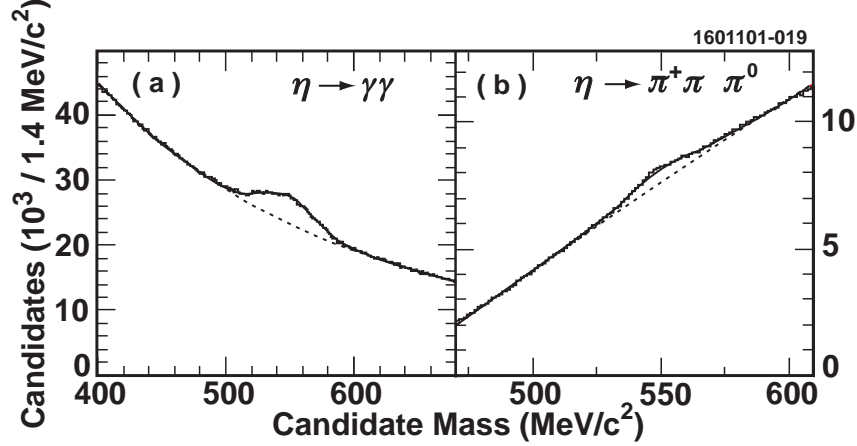
FIG. 3. The $\eta \to \gamma\gamma$ and $\eta \to \pi^+\pi^-\pi^0$ invariant mass distributions from data taken at or near the $\Upsilon(4S)$. The plots give the invariant mass distributions (histograms), which are each fit with the sum (solid lines) of a polynomial background (dashed lines) and a Gaussian signal.

at or just below the $\Upsilon(4S)$, recorded close in time to our $\Upsilon(1S)$ data. Before subtracting, we scaled the normalization of the $\pi^+\pi^-$ invariant mass distribution from the higher energy data by $\mathcal{L}/(s\epsilon)$ to take into account luminosity, the energy dependence of the cross section, and the reconstruction efficiency. We observe an excess of (29.4 ± 16.6) events for the $\Upsilon(1S)$ data in $0.45 \text{ GeV}/c^2 < m_{\pi\pi} < 1.1 \text{ GeV}/c^2$, consistent with zero excess.

We studied backgrounds to the $f_J(2220)$ in three ways. When we determined upper limits we used the smallest of the three, thereby being the most conservative. In two of these, we used the data sets taken at or just below the $\Upsilon(4S)$ and accepted candidates within a background box width $\pm 10\Gamma_f$ centered at m_f. To understand the relative rates of production for background events at the two energies ($\sqrt{s} = 9.46$ vs. 10.56 GeV), we first simulated the $udsc$ continuum, including initial state radiative effects, and for all events with a high-energy photon counted the number in which the invariant mass recoiling against the photon was within $\pm 2\Gamma_f$ for the $\Upsilon(1S)$ energy, or within $\pm 10\Gamma_f$ for the higher energy;[4] i.e., we did not fix the photon energy but rather the recoil mass region so that higher energy photons were involved in the events at $\sqrt{s} = 10.56$ GeV. The ratio of these numbers is 0.17 as compared to the naive correction factor of 0.2 from the ratio of box sizes; i.e., the relative production rate at the $\Upsilon(1S)$ is 86% of that at the higher energy.

If the dominant background in the signal region were from processes such as $e^+e^- \to \gamma\rho'$ or $e^+e^- \to \gamma\phi$, then the scaling would be as $1/s$. In that case the $\Upsilon(1S)$ probability would be 124% that of the higher energy data.

There may also be background contributions from other, as yet unmeasured, radiative $\Upsilon(1S)$ decays (e.g., $\Upsilon \to \gamma f_4(2050)$), which are not accounted for when comparing to the higher energy data. Therefore, as a third measure of the background, we look in the sidebands

---

[4]This is similar to the approach used in the study of $\Upsilon \to \eta\gamma \to \gamma\gamma\gamma$ described in the preceding section.

11

of the f_J region of the di-hadron spectra from the $\Upsilon(1S)$ data, namely $1.900\,\mathrm{GeV}/c^2 < m_{h\bar{h}} < 2.200\,\mathrm{GeV}/c^2$ and $2.264\,\mathrm{GeV}/c^2 < m_{h\bar{h}} < 2.500\,\mathrm{GeV}/c^2$. The number of events found in this region is then scaled by the ratio of the bin widths to predict the background in the signal region.

For the channel $f_J \to \pi^+\pi^-$, we observed one candidate in the $\pm 2\Gamma_f$ signal region of the $\Upsilon(1S)$ data set (see Figure 4a). There were eight events in the broader $\pm 10\Gamma_f$ box at the higher energies, which when scaled by luminosity, efficiency, and the production ratio (as obtained from $udsc$ simulations, described above) gave a mean background level in the signal box of $\mu_b(\pi\pi) = 0.12$ events. Using the $1/s$ scaling or the sideband technique yielded 0.17 and 0.36 events, respectively.

Similarly for the channel $f_J \to K^+K^-$ we found one event in the signal box in the $\Upsilon(1S)$ data (see Figure 4b). The analysis of the higher energy data showed 14 events in the $\pm 10\Gamma_f$ background region, distributed uniformly. When scaled appropriately for luminosity, efficiency, and production rate (as described above), this gave a mean background in the signal region of $\mu_b(KK) = 0.21$ events. Using the $1/s$ scaling or the sideband technique yielded 0.30 and 0.72 events, respectively.

The situation for $f_J \to p\bar{p}$ was different. Assigning proton masses to the two charged tracks moves the large peak from $e^+e^- \to \gamma\rho$ into the signal region. Although our selection criteria for conservation of four-momenta removed most of these backgrounds, we added a restriction that the time-of-flight as measured in the scintillation system be consistent for the two tracks to have proton masses, given their measured momenta. Also, nucleon-antinucleon annihilation can deposit large energies in the electromagnetic calorimeter, so our requirement on E/p would be very inefficient for anti-protons; therefore this requirement was removed for the negative track. The resulting distribution of $p\bar{p}$ invariant mass is shown in Figure 4c, having two candidate events in the signal box region of $\pm 2\Gamma_f$. In the higher energy data the background was no longer linear, due largely to the feed-through of $e^+e^- \to \gamma\rho$ events. We therefore fit this distribution to a Gaussian for this $\gamma\rho$ portion and a flat contribution. Integrating the fit result over the signal box region and correcting for relative efficiencies, integrated luminosities, and production (as described above) gave a mean background for this mode of $\mu_b(p\bar{p}) = 0.28$ events. A $1/s$ scaling would imply 0.40 events of background in the signal region, while the sideband technique gave a somewhat larger result of 0.48 events.

In analyzing these three decay modes, we found that the signal regions are kinematically distinct so that no events are common to any two of them.

To calculate reconstruction efficiencies we used our Monte Carlo simulations, based again on GEANT [19], with $\Upsilon \to \gamma f_J$ and $f_J \to h\bar{h}$ for each of $h = \pi^+, K^+, p$. The efficiencies, including possible systematic biases and uncertainties (as discussed below and summarized in Table III) and the statistics of the Monte Carlo samples, were $(28.8 \pm 4.2)\%$, $(21.9 \pm 3.8)\%$, and $(27.2 \pm 3.3)\%$, respectively.

The simulation of signal events was generated uniformly in $\cos\theta$ of the high-energy photon. Using the analysis for $J/\psi \to \gamma f_J$ with $J = 2$ [23] we have evaluated the range of possible angular distributions and their effect on our calculation of the geometric acceptance, assigning a systematic uncertainty of $\pm 10\%$. As in our search for $\Upsilon \to \gamma\eta$, we use previous detailed studies of low multiplicity $\tau^+\tau^-$ and $\gamma\gamma$ events to study uncertainties in track reconstruction and momentum measurement ($\pm 1.0\%$ per track) and trigger simulation ($\sim \pm 2.6\%$, and slightly dependent on momentum of the charged daughters). Also, as

before, we use previous CLEO experience [22] with radiative B meson decays to assess possible biases ($\pm2\%$) in our Υ invariant mass determination due to shower leakage and other calorimeter effects.

To evaluate the correctness of our simulations of the electron and muon rejection criteria, we analyzed charged pions from $\tau^- \to \rho^- \nu_\tau$ with $\rho^- \to \pi^-\pi^0$ (and charged conjugates) for both data and Monte Carlo. Using restrictive selection criteria on the masses of the π^0 and ρ^- mesons, on the specific ionization (dE/dx) of the charged pion, and the opening angle between the pions, we are left with a sample of charged tracks which is, according to the simulation, over 98% pions with less than 1% each of electrons and muons. Weighting the observed differences between simulation and data for these τ data by the momentum spectra of the pions in the f_J simulation shows that we need to increase our efficiencies by 2.6% and 9.9% due to the effects of the E/p and muon requirements, respectively. We also assigned a systematic uncertainty of that same magnitude for these possible biases. For the final states K^+K^- and $p\overline{p}$, we scaled these uncertainties by the relative inefficiencies for events to pass these two criteria in our signal simulation, as indicated in Table III. We note that the magnitude of the uncertainty stemming from the muon rejection criteria is similar to that from our prior work [2] on $\Upsilon \to \gamma\pi^+\pi^-$, which was $\pm13\%$, and calculated in an independent fashion.

To estimate the systematic uncertainties associated with possible mismodeling of the time-of-flight identification we followed the strategy used in our study [24] of $\gamma\gamma \to p\overline{p}$. Here we varied the widths of the timing distributions by $\pm20\%$, which is about four times the precision to which they are known. This changes the reconstruction efficiency by $\pm2\%$, which we assigned as the systematic uncertainty from this source.

TABLE III. Systematic uncertainty contributions, as relative percentages, to the efficiency for the studied decay modes for $\Upsilon \to \gamma f_J(2220)$. The combined uncertainties were obtained using quadrature addition.

Error source	$f_J \to \pi^+\pi^-$	$f_J \to K^+K^-$	$f_J \to p\overline{p}$
Angular distribution	10.0%	10.0%	10.0%
Trigger simulation	2.6%	2.6%	2.7%
Track reconstruction	2.0%	2.0%	2.0%
Υ mass distribution	2.0%	2.0%	2.0%
E/p criterion	2.6%	1.7%	0.3%
Muon suppression	9.9%	13.8%	5.7%
TOF identification	–	–	2.0%
Monte Carlo statistics	1.0%	1.2%	0.9%
Total (quadrature sum)	14.8%	17.6%	12.3%

To determine confidence limits for the results of this analysis, we followed the method advocated by Feldman and Cousins [25], which avoids under-coverage of confidence intervals. We adapted their method by replacing the confidence intervals for different mean numbers of observed events, μ, by confidence intervals for different values of the branching fraction, $\mathcal{B} = \mu/(N_\Upsilon\epsilon)$. The uncertainties in the efficiencies and in the number of $\Upsilon(1S)$ produced were

incorporated by smearing the central values with Gaussian distributions. Finally, we extend the confidence limits so that they cover the integer values allowed by Poisson statistics.

Before including systematic effects, we obtain 90% confidence intervals for the product $\mathcal{B}(\Upsilon \to \gamma f_J) \times \mathcal{B}(f_J \to h\overline{h})$ of $\mathcal{BB} < 10.2 \times 10^{-6}$ for $\pi^+\pi^-$, $\mathcal{BB} < 13.1 \times 10^{-6}$ for K^+K^-, and the range $0.7 \times 10^{-6} < \mathcal{BB} < 14.3 \times 10^{-6}$ for $p\overline{p}$. Note that for the $p\overline{p}$ case we have an interval with both lower and upper limits. After adding these systematic effects, we obtain $\mathcal{BB} < 12.0 \times 10^{-6}$ for $\pi^+\pi^-$, $\mathcal{BB} < 15.5 \times 10^{-6}$ for K^+K^-, and the range $0.5 \times 10^{-6} < \mathcal{BB} < 16.2 \times 10^{-6}$ for $p\overline{p}$. As noted earlier, we have used the estimate of the backgrounds, μ_b, as determined by the simulated production ratios. Using larger background estimates, such as from $1/s$ scaling or sideband comparisons, would give lower upper limits and eliminate the lower limit in the case of $f_J \to p\overline{p}$; for these three background estimates the probability of observing two or more events is between 3 and 8%, insufficiently small to claim a signal in this decay mode. We therefore take the conservative approach and quote the 90% confidence level upper limits as given and quote no lower limit for any of the channels. The results of our analysis are summarized in Table IV.

TABLE IV. Results of the search for $\Upsilon \to \gamma f_J$. The estimated background, obtained by scaling by the simulated continuum production rates, is the smallest of the three estimates of background levels and leads to the most conservative upper limits. The efficiencies and limits include systematic effects. The last row of entries is a scaling of the BES results for J/ψ decays.

	$f_J \to \pi^+\pi^-$	$f_J \to K^+K^-$	$f_J \to p\overline{p}$
Observed events in $\pm 2\Gamma_f$	1	1	2
Scaled continuum background (μ_b)	0.12	0.21	0.28
Overall efficiency	$(28.8 \pm 4.2)\%$	$(21.9 \pm 3.8)\%$	$(27.2 \pm 3.3)\%$
$\mathcal{B}(\Upsilon \to \gamma f_J)\times$ $\mathcal{B}(f_J(2220) \to h\overline{h})$ (90% C.L.)	$< 12.0 \times 10^{-6}$	$< 15.5 \times 10^{-6}$	$< 16.2 \times 10^{-6}$
$\mathcal{B}(J/\psi \to \gamma f_J)\times$ $\mathcal{B}(f_J(2220) \to h\overline{h}) \times 0.04$	$1.5^{+0.9}_{-0.8} \times 10^{-6}$	$2.5^{+1.2}_{-1.1} \times 10^{-6}$	$0.7 \pm 0.3 \times 10^{-6}$

As a comparison we have also computed the upper limits following the traditional approach of summing up the Poisson distribution $\mathcal{P}(\leq n \,|\, \mu) = e^{-\mu} \times (1 + \mu + ... + \frac{\mu^n}{n!})$ to 90% C.L. For $n = 1$ and 2, this gives limits of $\mu = 3.88$ and 5.32, respectively. Ignoring backgrounds the corresponding upper limits on the product branching fractions, including systematic effects, are $\mathcal{BB} < 9.3 \times 10^{-6}$ for $\pi^+\pi^-$, $\mathcal{BB} < 12.2 \times 10^{-6}$ for K^+K^-, and $\mathcal{BB} < 13.5 \times 10^{-6}$ for $p\overline{p}$. Note that this method can lead to under-coverage, as outlined in the paper by Feldman and Cousins [25].

V. COMPARISON TO PRIOR RESULTS AND THEORY

The only other reported analysis [1] of $\mathcal{B}(\Upsilon \to \gamma\eta)$ is by Crystal Ball [26], which determined a 90% C.L. upper limit of 3.5×10^{-4}; our limit of 2.1×10^{-5} is ~ 17 times more stringent.
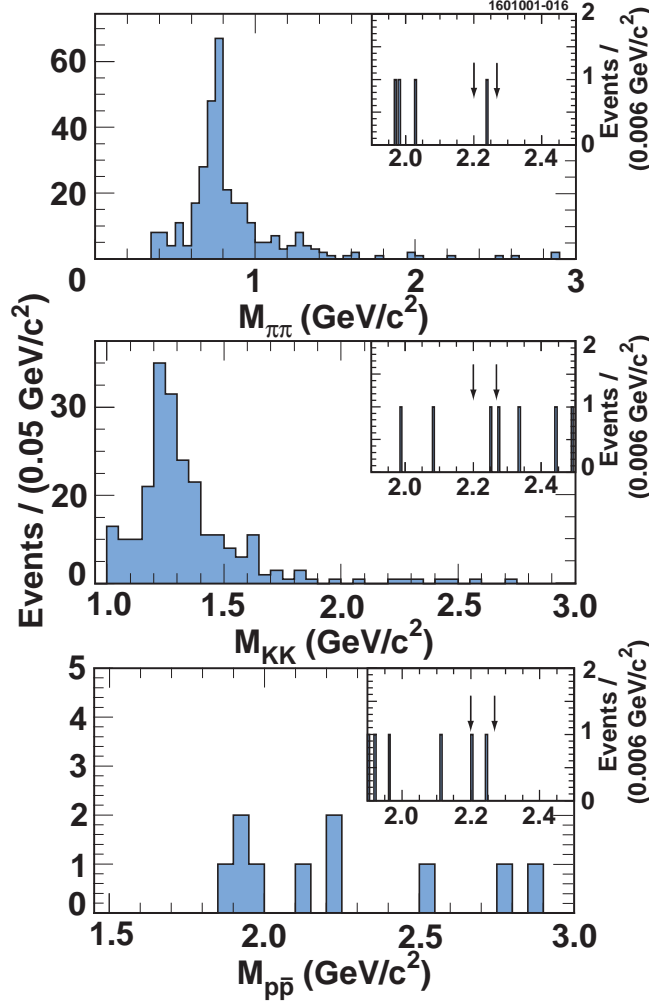
FIG. 4. Di-hadron invariant mass distributions for data events passing all selection criteria. The inserts show magnifications of the signal region. The vertical arrows in the inserts indicate the limits of the signal box, which are at $\pm 2\Gamma$, $\Gamma = 17$ MeV/c^2. No events are common to the signal regions of these channels.

We can then use our new limit on $\mathcal{B}(\Upsilon \to \gamma\eta)$, the measured enhancement [2] near 1270 MeV/c^2 in $\Upsilon \to \gamma\pi\pi$, and the measurements of $\mathcal{B}(J/\psi \to \gamma f_2(1270)) = (1.38 \pm 0.14) \times 10^{-3}$ and $\mathcal{B}(J/\psi \to \gamma\eta) = (0.86 \pm 0.08) \times 10^{-3}$ [1] to create interesting ratios. Here we assume that the observed structure in the di-pion mass spectrum near 1270 MeV/c^2 in the Υ study is totally due to f_2 production, which implies $\mathcal{B}(\Upsilon \to \gamma f_2(1270)) = (8.2 \pm 3.6) \times 10^{-5}$. We then obtain

$$R_f(\Upsilon, J/\psi) \equiv \frac{\mathcal{B}(\Upsilon \to \gamma f_2)}{\mathcal{B}(J/\psi \to \gamma f_2)} = 0.061 \pm 0.026 \quad \text{and} \tag{1}$$

$$R_\eta(\Upsilon, J/\psi) \equiv \frac{\mathcal{B}(\Upsilon \to \gamma\eta)}{\mathcal{B}(J/\psi \to \gamma\eta)} < 0.024 \ (90\% \ \text{C.L.}); \tag{2}$$

and, looking instead at the ratios of the two final states for a given vector parent,

15

$$R_{\Upsilon}(\eta, f_2) \equiv \frac{\mathcal{B}(\Upsilon \to \gamma\eta)}{\mathcal{B}(\Upsilon \to \gamma f_2)} < 0.32 \ (90\% \ \text{C.L.}) \quad \text{and} \tag{3}$$

$$R_{J/\psi}(\eta, f_2) \equiv \frac{\mathcal{B}(J/\psi \to \gamma\eta)}{\mathcal{B}(J/\psi \to \gamma f_2)} = 0.62 \pm 0.09. \tag{4}$$

These results were obtained by including the various uncertainties in a Monte Carlo technique. In the last two of the ratios, we assume that all the uncertainties from the J/ψ and Υ measurements are uncorrelated. Our limits show that the branching fractions into $\gamma\eta$ and $\gamma f_2(1270)$ behave differently in the cases of J/ψ and Υ, although not as dramatically as in the case of $\Upsilon \to \gamma\eta'$ [3]. In addition we form the double ratio:

$$\mathcal{R} \equiv \frac{R_{\Upsilon}(\eta, f_2)}{R_{J/\psi}(\eta, f_2)} = \frac{\mathcal{B}(\Upsilon \to \gamma\eta)}{\mathcal{B}(\Upsilon \to \gamma f_2)} \times \frac{\mathcal{B}(J/\psi \to \gamma f_2)}{\mathcal{B}(J/\psi \to \gamma\eta)} < 0.53 \tag{5}$$

at 90% C.L. This is to be compared with the prediction of Körner *et al.* [4] of

$$\mathcal{R}_{theory} = \frac{0.10}{0.24} = 0.42; \tag{6}$$

Chao's technique [10] first calculates mixing angles among the various pseudoscalars, extending the $J^{PC} = 0^{-+}$ nonet to include heavier cousins such as the η_b. Then, using the predicted allowed M1 transition $\Upsilon \to \gamma\eta_b$, Chao predicts $\mathcal{B}(\Upsilon \to \gamma\eta) = 1 \times 10^{-5}$, which is consistent with our limit. We note that in our prior work [3] we did not know of Chao's prediction of $\mathcal{B}(\Upsilon \to \gamma\eta') = 6 \times 10^{-5}$, which is to be compared with our upper limit for that process of 1.6×10^{-5} at 90% C.L.

Intemann's extended vector dominance model gives $6.5 \times 10^{-8} < \mathcal{B}(\Upsilon \to \gamma\eta) < 1.2 \times 10^{-7}$, with the two limits determined by having destructive or constructive interference, respectively, between the terms involving Υ and Υ'. This range of predictions is well below our new limit. Ma uses a technique in which the decay amplitude factorizes into a non-relativistic piece describing the bound state of the heavy quarkonium and an expansion in "twist" to characterize the conversion of the gluons into the final state meson. The published value [11] was $\mathcal{B}(\Upsilon \to \gamma\eta) = 1.2 \times 10^{-7}$, although subsequent correspondence [27] indicates the correct value is actually 3.3×10^{-7}. In either case, these are significantly below our limit. Feldmann *et al.* [9] predict the ratio $\Gamma(\Upsilon \to \gamma\eta')/\Gamma(\Upsilon \to \gamma\eta) = 6.5$. Given that we only have limits on these two processes, we cannot address their prediction.

For the glueball candidate, our 90% C.L. limits on the product branching fractions $\mathcal{B}(\Upsilon \to \gamma f_J) \times \mathcal{B}(f_J \to h\overline{h})$ are on the order of 1.5×10^{-5} for each of the three modes. In Table IV we show the results from BES [12] for these channels in radiative J/ψ decay, scaled by a factor of $\mathcal{F}$. This scaling arises from the naive expectation that the amplitude for the radiative process of meson formation varies directly as the quark charge (to couple to the photon) and inversely as the quark mass (from the fermionic propagator between the photon emission and the resonance formation). One then squares this to get the rate and corrects for the full widths of the heavy quarkonia [1] to obtain

$$\mathcal{F} = (\frac{q_b m_c}{q_c m_b})^2 \cdot \frac{\Gamma_{J/\psi}}{\Gamma_{\Upsilon}} = 0.04. \tag{7}$$

16

Here we have used masses of 1.7 GeV/c^2 and 5.2 GeV/c^2 for the charm and bottom quarks, respectively. As shown in Table IV and in Figure 5, our limits on radiative $f_J(2220)$ production do not confront these predictions.

As a quantification of this situation, we have have used a Monte Carlo technique to evaluate the ratio of the CLEO and BES [12] results, $i.e.,$

$$R_{f_J}(\Upsilon, J/\psi) \equiv \frac{\mathcal{B}(\Upsilon \to \gamma f_J)}{\mathcal{B}(J/\psi \to \gamma f_J)} = \frac{\mathcal{B}(\Upsilon \to \gamma f_J) \cdot \mathcal{B}(f_J \to h\overline{h})}{\mathcal{B}(J/\psi \to \gamma f_J) \cdot \mathcal{B}(f_J \to h\overline{h})}. \tag{8}$$

For the denominator we add the BES statistical and systematic uncertainties in quadrature and throw BES "experiments" in a Gaussian distribution, keeping only physical values. In all three cases ($h = \pi^+, K^+, p$) we can only say that R_{f_J} is less than roughly 0.50 at 90% C.L., an order of magnitude from the predicted ratio of $\mathcal{F} = 0.04$.

We also note that the Crystal Barrel [17] collaboration has combined their results with those of BES [12] to obtain that $\mathcal{B}(J/\psi \to \gamma f_J(2220)) > 0.003$ at 95% C.L. Applying the naive scaling factor $\mathcal{F}$ would then predict that $\mathcal{B}(\Upsilon \to \gamma f_J(2220)) > 1.2 \times 10^{-4}$; this would be larger than the CLEO result [2] for the radiative decay to $f_2(1270)$.

VI. SUMMARY AND ACKNOWLEDGMENTS

In summary, we have used the CLEO detector operating at the CESR storage ring to search for two-body radiative $\Upsilon(1S)$ decays. In the work presented in this Article, we reported specifically on searches for the decay $\Upsilon \to \gamma\eta$ with the subsequent decays $\eta \to \pi^0\pi^0\pi^0$, $\eta \to \pi^+\pi^-\pi^0$, and $\eta \to \gamma\gamma$ and for the decay $\Upsilon \to \gamma f_J(2220)$ with the subsequent decays of the glueball candidate of $f_J \to \pi^+\pi^-$, $f_J \to K^+K^-$, and $f_J \to p\overline{p}$. Including our prior published results we have the following:

for the decay $\Upsilon \to \gamma\pi\pi$ [2],

$$\mathcal{B}(\Upsilon \to \gamma\pi^+\pi^-) = (6.3 \pm 1.2 \pm 1.3) \times 10^{-5} \ \ [m_{\pi\pi} > 1.0 \text{ GeV}/c^2] \ ,$$

and

$$\mathcal{B}(\Upsilon \to \gamma\pi^0\pi^0) = (1.7 \pm 0.6 \pm 0.3) \times 10^{-5} \ \ [m_{\pi\pi} > 1.0 \text{ GeV}/c^2] \ ;$$

and, assuming the enhancement in the invariant mass spectrum for $\pi^+\pi^-$ in the region of 1.3 GeV/c^2 is due to $f_2(1270)$ production,

$$\mathcal{B}(\Upsilon \to \gamma f_2(1270)) = (8.2 \pm 3.6) \times 10^{-5};$$

for the decay $\Upsilon \to \gamma\eta'$ [3],

$$\mathcal{B}(\Upsilon \to \gamma\eta') < 1.6 \times 10^{-5} \ \ [90\%\text{C.L.}];$$

for the decay $\Upsilon \to \gamma\eta$,

$$\mathcal{B}(\Upsilon \to \gamma\eta) < 2.1 \times 10^{-5} \ \ [90\%\text{C.L.}];$$

and for the product branching fractions involving the glueball candidate $f_J(2220)$,

$$\mathcal{B}(\Upsilon \to \gamma f_J) \times \mathcal{B}(f_J \to \pi^+\pi^-) < 1.2 \times 10^{-5} \ \ [90\%\text{C.L.}],$$

$$\mathcal{B}(\Upsilon \to \gamma f_J) \times \mathcal{B}(f_J \to K^+K^-) < 1.6 \times 10^{-5} \quad [90\%\text{C.L.}],$$

and

$$\mathcal{B}(\Upsilon \to \gamma f_J) \times \mathcal{B}(f_J \to p\overline{p}) < 1.6 \times 10^{-5} \quad [90\%\text{C.L.}].$$

We also present this summary in graphical form in Figure 5: (*i*) the world-average [1] values for the radiative two-body decays of the J/ψ to η, η', and $f_2(1270)$; (*ii*) the BES [12] results for the product branching fractions $\mathcal{B}(J/\psi \to \gamma f_J) \times \mathcal{B}(f_J \to h^+h^-)$; (*iii*) the scaling of these J/ψ results by $\mathcal{F}$ to obtain estimates for the corresponding $\Upsilon(1S)$ decays; (*iv*) the CLEO results summarized above; and (*v*) theoretical predictions from Körner *et al.* [4], Intemann [6], Ma [11], and Chao [10].
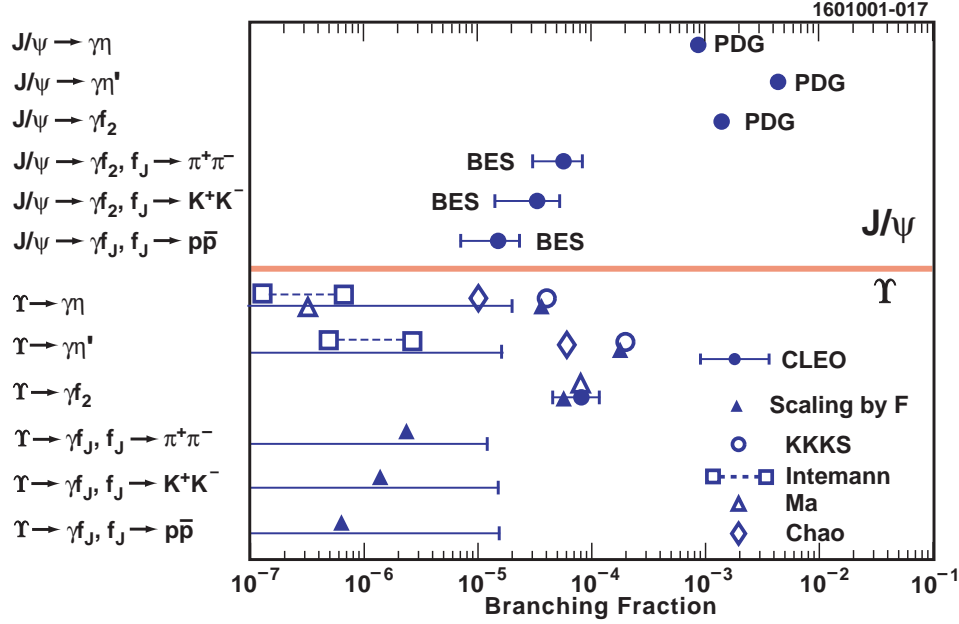

FIG. 5. Radiative decays of J/ψ and $\Upsilon(1S)$ vector mesons. Shown are the experimental results (as solid circles or limit bars) from the PDG for the well-established radiative J/ψ decays to η, η', and $f_2(1270)$, from BES for the three charged modes of radiative decay to the glueball candidate $f_J(2220)$, and from CLEO for the Υ decays. The solid triangles give the values for radiative Υ decay based on radiative J/ψ decay and the naive scaling involving the masses and charges of the constituent quarks. Various explicit theoretical predictions for the radiative production of η, η', and $f_2(1270)$ are shown as open symbols. For references see the text.

18

REFERENCES

[1] D.E. Groom *et al.* (Particle Data Group), E. Phys. J. C **15**, 1 (2000).

[2] A. Anastassov *et al.* (CLEO Collaboration), Phys. Rev. Lett. **82**, 286 (1999).

[3] S. Richichi *et al.* (CLEO Collaboration), Phys. Rev. Lett. **87**, 141801 (2001).

[4] J.G. Körner, J.H. Kühn, M. Krammer and H. Schneider, Nucl. Phys. B **229**, 115 (1983).

[5] J.H. Kühn, Phys. Lett. B **127**, 257 (1983).

[6] G.W. Intemann, Phys. Rev. D **27**, 2755 (1983).

[7] V.N. Baier and A.G. Grozin, Nucl. Phys. B **192**, 476 (1981).

[8] P. Ball, J.-M. Frère and M. Tytgat, Phys. Lett. B **365**, 367 (1996).

[9] Th. Feldmann, P. Kroll, and B. Stech, Phys. Lett. B **449**, 339 (1999).

[10] Kuang-Ta Chao, Nucl. Phys. **B335**, 101 (1990); Nucl. Phys. **B317**, 597 (1989).

[11] J.P. Ma, Nucl. Phys. **B605**, 625 (2001).

[12] J.Z. Bai *et al.* (BES Collaboration), Phys. Rev. Lett. **76**, 3502 (1996).

[13] J.Z. Bai *et al.* (BES Collaboration), Phys. Rev. Lett. **81**, 1179 (1998).

[14] Li Jin, in 'Proceedings of the 28th International Conference on High Energy Physics, Warsaw, Poland', p. 504 (1996).

[15] R. Godang *et al.* (CLEO Collaboration), Phys. Rev. Lett. **79**, 3829 (1997); M.S. Alam *et al.* (CLEO Collaboration), Phys. Rev. Lett. **81**, 3328 (1998).

[16] C. Evangelista *et al.* (JETSET Collaboration), Phys. Rev. D **56**, 3803 (1997) and Phys. Rev. D **57**, 5370 (1998);

[17] C. Amsler *et al.* (Crystal Barrel Collaboration), Phys. Lett. B**520**, 175 (2001).

[18] Y. Kubota *et al.* (CLEO Collaboration), Nucl. Instrum. Methods **A320**, 66 (1992).

[19] R. Brun *et al.*, GEANT3.15, CERN Report DD/EE/84-1 (1987).

[20] C. Bebek *et al.*, Nucl. Instrum. Methods **A302**, 261 (1991).

[21] M. Procario *et al.* (CLEO Collaboration), Phys. Rev. Lett. **70**, 1207 (1993); R. Balest *et al.* (CLEO Collaboration), Phys. Rev. Lett. **75**, 3809 (1995).

[22] T.E. Coan *et al.* (CLEO Collaboration), Phys. Rev. Lett. **84**, 5283 (2000).

[23] K.F. Einsweiler, 'Radiative Decays of the $\psi(3097)$ to Two Meson Final States', Ph.D. Thesis, SLAC-272, UC-34D, May 1984 (unpublished; available on SPIRES).

[24] M. Artuso *et al.* (CLEO Collaboration), Phys. Rev. D **50**, 5484 (1994).

[25] G.J. Feldman and R.D. Cousins, Phys. Rev. D **57**, 3873 (1998).

[26] P. Schmitt *et al.* (Crystal Ball Collaboration), Z. Phys. C **40**, 199 (1988).

[27] J.P. Ma, private communication, July 2001; *erratum*, Nucl. Phys. **B611**, 523 (2001).